Int. J. Solids Structures Vol. 27, No. 6, pp. 751–767, 1991
Printed in Great Britain.

0020–7683/91 $3.00+ .00

EFFECTIVE WAVE VELOCITY AND ATTENUATION IN A MATERIAL WITH DISTRIBUTED PENNY-SHAPED CRACKS

CH. ZHANG† and J. D. ACHENBACH
Center for Quality Engineering and Failure Prevention, Northwestern University, Evanston, IL 60208-3020, U.S.A.

(*Received* 15 *August* 1989; *in revised form* 6 *April* 1990)

Abstract—Wave propagation in a material containing distributed penny-shaped cracks was investigated. An improved approach was developed for calculating the phase velocity and the attenuation of ultrasonic waves. In this approach, the effects of neighboring cracks on a reference crack are approximated by the effects of triads of double forces of strengths proportional to the crack opening volumes, and located at the geometrical centers of the cracks. The averaged crack opening displacements and crack opening volumes of the reference crack are split into two terms. The first term corresponds to the quantities induced by the interaction of the single reference crack with an incident wave, while the second term represents the interaction between this reference crack and neighboring cracks. The averaged crack opening displacements are used in calculating the forward scattering amplitude, from which the phase velocity and the coefficient of attenuation are subsequently computed. The present analysis was limited to parallel cracks and to low frequencies, but the principle can be used for more general cases. Since crack interactions have been taken into account, the analysis provides a better approximation than the standard approach proposed by Foldy (1945, *Phys. Rev.* 67, 107–119), especially for intermediate and large crack densities.

1. INTRODUCTION

Analytical considerations combined with experimental observations of the velocity and the attenuation of ultrasonic waves in a damaged material, provide a means of characterizing the damaged state of the material. Often, a decrease in the velocity or an increase in the attenuation of ultrasonic waves is an indication of stiffness degradation and/or loss of strength of the material. In this paper, an advanced analysis of both the effective wave velocity and the attenuation coefficient is presented, for a material whose damaged state is caused by a distribution of penny-shaped cracks.

Wave propagation in a material containing distributed defects (such as cracks, voids or inclusions) often involves multiple scattering. In the independent scatterer approximation, the interaction between individual scatterers is ignored. This approximation is acceptable for a dilute distribution or for weak scatterers; it may not be good enough for a dense distribution or for strong scatterers. A heuristic approximation for multiple scattering was proposed by Foldy (1945), who obtained a closed form expression for the wavenumber of the coherent wave (Foldy's equation). An improved approach, the quasicrystalline approximation, which involves two-particle correlations was developd by Lax (1952). For reasons of simplicity, the independent scatterer approximation and Lax's quasicrystalline approximation have been generally used, see Waterman and Truell (1961), Twersky (1962), Bose and Mal (1974), Datta (1977), Varadan *et al.* (1978), Datta *et al.* (1980), Sayers and Smith (1983), Gubernatis and Domany (1984) and Varadan *et al.* (1985). For spherical voids, special forms of two-particle correlations which give a better approximation for high densities of voids have been used by Varadan *et al.* (1985). However, for scatterers that are of a complicated geometry, such as penny-shaped cracks, ellipsoidal voids or inclusions, such correlation functions do not yet exist.

In this paper, a novel method is presented which is based on the approach developed by Sotiropoulos and Achenbach (1988) to account for the interaction effects between cracks. For simplicity, the cracks are assumed to be of the same size and to be oriented parallel to each other. The effects of neighboring cracks on an arbitrarily selected crack (reference

† Department of Engineering Mechanics, Tongji University, Shanghai, P.R. China.

crack) are represented by systems of dipoles at the geometrical centers of the neighboring cracks. The crack-opening displacements of the reference crack then split into two parts: the first part is due to the incident wave in the absence of other cracks, while the second part is induced by the presence of all other cracks. By taking configurational averages of all quantities, the average forward scattering amplitude is calculated by substituting the average crack-opening displacements into the far-field expressions of the scattered displacements. Subsequent substitution of the average forward scattering amplitude into Foldy's dispersion equation leads to an expression for the effective complex wavenumber. The first two terms of this expression correspond to the standard form of Foldy's approximation, while the third term is an additional term which accounts for crack interaction effects. The effective wave velocity and the coefficient of attenuation are then calculated from the imaginary part and the real part of the complex wave number, respectively. Numerical calculations show that for very small crack densities the results from the standard and the modified approach agree, while for larger crack densities substantial deviations can occur.

The present paper is limited to low-frequency (long wavelength) scattering of time-harmonic, plane longitudinal waves (L-waves). The principle used can, however, be extended to moderate or high frequencies.

In Section 2, the scattering of a plane L-wave by a single penny-shaped crack is reviewed. Results in the low-frequency range for the crack-opening displacements and the forward scattering amplitude are summarized. A perturbation technique is applied to obtain closed form solutions. The method used by Sotiropoulos and Achenbach (1988) for calculating the multiple scattering effect for a distribution of coplanar cracks, is extended in Section 3 to a 3-D distribution of penny-shaped cracks. In subsequent sections the standard Foldy's equation and the improved one, are presented and numerical results are given.

It is assumed in this analysis that the size of the cracks and the characteristic wavelengths are much larger than the characteristic dimensions of the microstructure of the material, so that wave scattering by microstructures can be ignored.

Previous studies of wave propagation in a randomly cracked material can be found in the papers by Garbin and Knopoff (1973, 1975a,b), and McCarthy and Carroll (1984), who calculated the elastic moduli of a cracked medium; and by O'Connell and Budiansky (1974) who calculated the wave velocity by using a self-consistent static approach. Wave attenuation in a cracked material has been investigated by Piau (1979) and by Chatterjee *et al.* (1980). The effects of anisotropy on the effective elastic moduli and attenuation have been investigated by Anderson *et al.* (1974) and Piau (1980).

2. SCATTERING BY A PENNY-SHAPED CRACK

We consider a penny-shaped crack in an infinite, homogeneous, isotropic and linearly elastic solid, as shown in Fig. 1. An incident time harmonic, plane longitudinal wave of the form

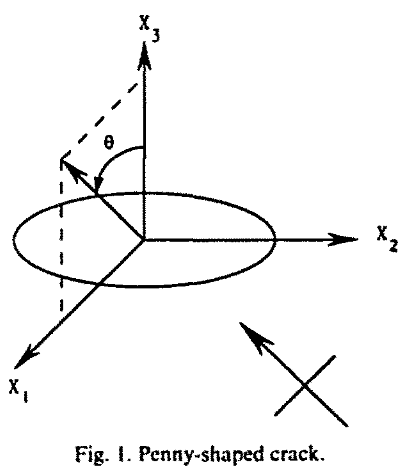

Fig. 1. Penny-shaped crack.

$$u_i^{\text{in}} = \begin{Bmatrix} \sin\theta \\ 0 \\ \cos\theta \end{Bmatrix} e^{ik_L(x_1 \sin\theta + x_3 \cos\theta)} \tag{1}$$

interacts with the crack and generates scattered waves. The amplitude of the incident wave is unity, and its propagation direction is taken in the x_1x_3 plane. Also, θ is the angle of incidence and k_L is the wave number of the incident wave. We assume that the faces of the crack will not touch. The boundary conditions on the faces of the crack then are

$$\sigma_{3q}^{\text{in}}(\mathbf{x}) + \sigma_{3q}^{\text{sc}}(\mathbf{x}) = 0, \quad \mathbf{x} \in A^{\pm}, \tag{2}$$

where σ_{3q}^{in} represents the stress components due to the incident wave in the absence of the crack, σ_{3q}^{sc} denotes the stress components of the scattered wave induced by the interaction of the incident wave with the crack, and $A^{\pm}$ are the insonified and shadow sides of the crack.

The scattered displacement field can be expressed by the following representation integral

$$u_k^{\text{sc}}(\mathbf{x}) = \int_{A^+} \sigma_{ijk}^G(\mathbf{x};\mathbf{y}) \Delta u_i(\mathbf{y}) n_j \, \mathrm{d}S(\mathbf{y}), \quad \mathbf{x} \notin A^+, \tag{3}$$

in which $\mathbf{x}$ denotes the position vector of the observation point; $\mathbf{y}$ denotes the position vector of the source point; n_j is the unit normal vector of A^+; and Δu_j are the crack-opening displacements (displacement jumps across the crack faces) defined by

$$\Delta u_j(\mathbf{y}) = u_j|_{\mathbf{y} \in A^+} - u_j|_{\mathbf{y} \in A^-} \; ; \tag{4}$$

and σ_{ijk}^G is the stress Green's function of the uncracked medium. The function σ_{ijk}^G denotes the stress components at position $\mathbf{x}$ due to a time-harmonic, unit point force applied at position $\mathbf{y}$ in the direction y_k.

By substituting (3) into Hooke's law

$$\sigma_{pq} = C_{pqkl} u_{k,l}, \tag{5}$$

and by using the boundary conditions (2), the following system of boundary integral equations can be obtained

$$\sigma_{3q}^{\text{in}}(\mathbf{x}) = -C_{3qkl} \frac{\partial}{\partial x_l} \int_{A^+} \sigma_{ijk}^G(\mathbf{x};\mathbf{y}) \Delta u_i(\mathbf{y}) n_j \, \mathrm{d}S(\mathbf{y}), \quad \mathbf{x} \in A^+. \tag{6}$$

Here C_{pqkl} is the elastic tensor which for an isotropic material is given by

$$C_{pqkl} = \lambda \delta_{pq} \delta_{kl} + \mu(\delta_{pk} \delta_{ql} + \delta_{pl} \delta_{qk}), \tag{7}$$

where λ, μ are Lamé's elastic constants and δ_{pq} is the Kronecker delta. Closed form solutions to eqn (6) cannot be obtained and, in general, a suitable numerical method must be employed. Among many studies of this problem we mention the works by Martin and Wickham (1983), Lin and Keer (1987), Budreck and Achenbach (1988), and Nishimura and Kobayashi (1989). Earlier studies of elastic wave scattering by a penny-shaped crack have been presented by Robertson (1967), Mal (1970), Garbin and Knopoff (1973) and Krenk and Schmidt (1982), who used integral transform and dual integral equations techniques.

In this paper we restrict our analysis to the low-frequency range where approximate solutions to eqn (6) can be obtained. This can be done, for example, by the perturbation technique proposed by Roy (1987), who investigated the elastic wave scattering by an elliptic crack. In this procedure, the known and unknown quantities of eqn (6) are expanded into a power series of ik_T as

$$\sigma_{3q}^{in}(\mathbf{x}) = \mu \sum_{m=0}^{\infty} \frac{(ik_T)^m}{m!} \sigma_{3q}^{(m)}(x_1 \sin\theta)^m, \tag{8}$$

$$\sigma_{ijk}^{G}(\mathbf{x};\mathbf{y}) = \mu \sum_{m=0}^{\infty} \frac{(ik_T)^m}{m!} \sigma_{ijk}^{(m)}(\mathbf{x};\mathbf{y}), \tag{9}$$

$$\Delta u_i(\mathbf{x}) = \sum_{m=0}^{\infty} \frac{(ik_T)^m}{m!} \Delta u_i^{(m)}(\mathbf{x}), \tag{10}$$

where k_T is the wavenumber of transverse waves; and $\sigma_{3q}^{(m)}$, $\sigma_{ijk}^{(m)}$ and $\Delta u_i^{(m)}$ are expansion coefficients. Substituting (8)–(10) into (6) and collecting terms of the same order in k_T, yields a system of integral equations which can be solved analytically. Without going into details we summarize in the following, the final results for the crack-opening displacements. A detailed analysis has been given by Roy (1987).

In the low-frequency range, the crack-opening displacements have the form

$$\Delta u_i(\mathbf{x}) = \sum_{m=0}^{3} \frac{(ik_T)^m}{m!} \Delta u_i^{(m)}(\mathbf{x}) + O(k_T a)^4 \tag{11}$$

where a is the radius of the crack, and

$$\Delta u_i^{(0)}(\mathbf{x}) = a_i^{(0)}\psi(\mathbf{x}), \tag{12}$$

$$\Delta u_i^{(1)}(\mathbf{x}) = (a_i^{(1)}x_1 + b_i^{(1)}x_2)\psi(\mathbf{x}), \tag{13}$$

$$\Delta u_i^{(2)}(\mathbf{x}) = (a_i^{(2)} + b_i^{(2)}x_1^2 + C_i^{(2)}x_2^2 + d_i^{(2)}x_1x_2)\psi(\mathbf{x}), \tag{14}$$

$$\Delta u_i^{(3)}(\mathbf{x}) = (a_i^{(3)} + b_i^{(3)}x_1 + C_i^{(3)}x_2 + d_i^{(3)}x_1^3 + e_i^{(3)}x_2^3 + f_i^{(3)}x_1^2x_2 + g_i^{(3)}x_1x_2^2)\psi(\mathbf{x}). \tag{15}$$

Here

$$\psi(\mathbf{x}) = \sqrt{a^2 - (x_1^2 + x_2^2)}, \tag{16}$$

and expressions for the coefficients $a_i^{(m)}, b_i^{(m)}, \ldots, g_i^{(m)}$ in terms of the functions $\sigma_{3q}^{(m)}$, can be found in Appendix 3 of Roy (1987). According to Roy (1987) and Mal (1972) this approximation is valid for at least $k_T a < 0.6$. Figure 2 shows a comparison of V_3/a^2u_0 with

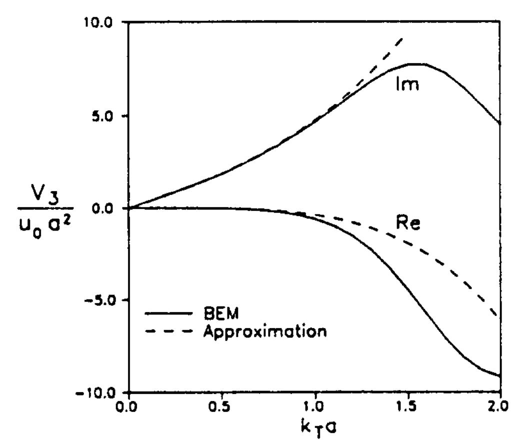

Fig. 2. Crack-opening volume as a function of $k_T a$.

numerically exact results which were obtained by a boundary element solution of eqn (6) for normal incidence of a longitudinal wave of amplitude u_0. Here V_3 is the crack-opening volume, i.e. the integral of $\Delta u_3(\mathbf{x})$ over the area of the crack, see eqn (37). It is noted that a very adequate approximate solution is obtained for values of $k_T a$ up to $k_T a = 1$.

A representation formula for the scattered far-field ($|\mathbf{x}| \gg |\mathbf{y}|$) can be obtained by simplifying eqn (3) with the approximation

$$|\mathbf{x}-\mathbf{y}| = |\mathbf{x}| - \hat{\mathbf{x}}\cdot\mathbf{y}, \tag{17}$$

where $\hat{\mathbf{x}}$ is the unit vector along $\mathbf{x}$. Introducing a spherical coordinate system

$$x_1 = R\sin\theta\cos\phi, \quad x_2 = R\sin\theta\cos\phi, \quad x_3 = R\cos\theta, \tag{18}$$

and substituting (17) into (3), the following results are obtained

$$u_l^{sc}(R,\theta,\phi) = F_l(\theta,\phi)\frac{\exp(ik_l R)}{R}, \quad l = R,\theta,\phi, \tag{19}$$

where

$$k_l = \begin{cases} k_L, & \text{for } l = R \\ k_T, & \text{for } l = \theta,\phi; \end{cases} \tag{20}$$

$$F_R(\theta,\phi) = -\frac{ik_L}{2}\{(1-2\kappa^2\sin^2\theta)I_z(k_L\sin\theta) + \kappa^2\sin 2\theta\, I_c(k_L\sin\theta)\}, \tag{21}$$

$$F_\theta(\theta,\phi) = \frac{ik_T}{2}\{\sin 2\theta\, I_z(k_T\sin\theta) - \cos 2\theta\, I_c(k_T\sin\theta)\}, \tag{22}$$

$$F_\phi(\theta,\phi) = \frac{ik_T}{2}\cos\theta\, I_S(k_T\sin\theta), \tag{23}$$

$$I_z(\lambda) = \frac{1}{2\pi}\int_0^{2\pi}\int_0^a \Delta u_3(r,\phi)\exp(-i\lambda r\cos\chi)r\,dr\,d\phi, \tag{24}$$

$$I_c(\lambda) = \frac{1}{2\pi}\int_0^{2\pi}\int_0^a [\Delta u_r(r,\phi)\cos\chi + \Delta u_\phi(r,\phi)\sin\chi]\exp(-i\lambda r\cos\chi)r\,dr\,d\phi, \tag{25}$$

$$I_s(\lambda) = \frac{1}{2\pi}\int_0^{2\pi}\int_0^a [\Delta u_r(r,\phi)\sin\chi - \Delta u_\phi(r,\phi)\cos\chi]\exp(-i\lambda r\cos\chi)r\,dr\,d\phi, \tag{26}$$

$$\chi = \theta - \phi. \tag{27}$$

In eqns (25) and (26), Δu_r and Δu_ϕ are the crack-opening displacements in the polar coordinate system. In the case of L-wave incidence, only the forward scattered L-wave amplitude F_R is important for the determination of the effective wave velocity (phase-velocity) and the attenuation. Thus in the following, only F_R is calculated explicitly. This can easily be done by substituting the crack-opening displacements, eqns (11)–(16), into eqns (21), (24) and (25). The final result for $\phi = 0$ is

$$F_R(\theta,0) = \frac{k_L^2 a^3}{3\pi k}\left\{\frac{(1-2\kappa^2\sin^2\theta)^2}{\kappa(1-\kappa^2)}F_1 - \frac{4\kappa^3\sin 2\theta}{3-2\kappa^2}F_2\right\}, \tag{28}$$

where

$$F_\alpha = a_\alpha^0 - \frac{(k_L a)^2}{10\kappa^2}(a_\alpha^0\kappa^2\sin^2\theta + 2a_\alpha^1\kappa\sin\theta + 5a_\alpha^2 + a_\alpha^3 + a_\alpha^4) - \frac{i(k_L a)^3}{6\kappa^3}a_\alpha^5 + O[(k_L a)^4], \quad \alpha = 1,2. \tag{29}$$

The coefficients a_α^i ($i = 0, 1, \ldots, 5$; $\alpha = 1, 2$) are listed in Appendix B.

3. INTERACTION OF DISTRIBUTED PARALLEL PENNY-SHAPED CRACKS

Parallel penny-shaped cracks of the same radius a are considered, and it is assumed that the cracks are randomly distributed. When the cracks are sufficiently closely spaced, wave propagation in such a solid involves multiple scattering. In this section we extend the technique of Sotiropoulos and Achenbach (1988) for multiple scattering of elastic waves by an array of collinear cracks, to wave scattering by a volumetric distribution of penny-shaped cracks. Special attention is devoted to the determination of the average crack-opening displacements of a reference crack because these quantities play a fundamental role in estimating the scattered far-field.

If the total number of cracks in a bounded region is N, then the scattered displacement field can be represented by [see also eqn (3)]

$$u_k^{sc}(\mathbf{x}) = \sum_{p=1}^{N}\int_{A_p^+}\sigma_{ijk}^G(\mathbf{x};\mathbf{y})\Delta u_i^p(\mathbf{y})n_j\,\mathrm{d}S(\mathbf{y}), \quad \mathbf{x}\in\sum_{p=1}^{N}A_p^+, \tag{30}$$

where A_p^+ denotes the insonified area and Δu_i^p represents the crack-opening displacements of the pth crack. The corresponding representation integral for the scattered stress components is obtained by substituting eqn (30) into Hooke's law. This results in

$$\sigma_{3l}^{sc}(\mathbf{x}) = \sum_{p=1}^{N} C_{3lkl}\frac{\partial}{\partial x_l}\int_{A_p^+}\sigma_{ijk}^G(\mathbf{x};\mathbf{y})\Delta u_i^p(\mathbf{y})n_j\,\mathrm{d}S(\mathbf{y}), \quad \mathbf{x}\notin\sum_{p=1}^{N}A_p^+. \tag{31}$$

We could follow the same procedure as discussed in the last section to obtain a system of $3N$ integral equations, by letting $\mathbf{x}\to A_p^+$ and by considering the stress-free boundary conditions on the pth crack. However, for large N this method becomes impractical for the determination of the crack-opening displacements because of the enormous computational effort. Here we will use the method proposed by Sotiropoulos and Achenbach (1988) to obtain an approximate solution for the crack-opening displacements.

The basic idea of this approximation is to split Δu_i^p into two parts

$$\Delta u_i^p(\mathbf{y}) = \Delta u_i^{p0}(\mathbf{y}) + \sum_{\substack{q=1\\ q\neq p}}^{N}\Delta u_i^{pq}(\mathbf{y}), \tag{32}$$

in which the first part denotes the crack-opening displacement caused by the incident wave in the absence of all other cracks, and the second part represents the crack-opening displacement due to the presence of all other cracks. In particular, the term Δu_i^{pq} represents the influence of the qth crack on the crack-opening displacements of the pth crack. Substituting eqn (32) into eqn (31) and applying the boundary conditions on the pth crack, yields the following separate equations

$$C_{3ikl}\frac{\partial}{\partial x_l}\int_{A_p^+}\sigma_{ijk}^G(\mathbf{x};\mathbf{y})\Delta u_i^{p0}(\mathbf{y})n_j\,\mathrm{d}S(\mathbf{y}) = -\sigma_{3i}^{\mathrm{in}}(\mathbf{x}),\quad \mathbf{x}\in A_p^+,\tag{33}$$

$$C_{3ikl}\frac{\partial}{\partial x_l}\int_{A_p^+}\sigma_{ijk}^G(\mathbf{x};\mathbf{y})\Delta u_i^{pq}(\mathbf{y})n_j\,\mathrm{d}S(\mathbf{y}) = -C_{3ikl}\frac{\partial}{\partial x_l}\int_{A_q^+}\sigma_{ijk}^G(\mathbf{x};\mathbf{y})\Delta u_i^{q}(\mathbf{y})n_j\,\mathrm{d}S(\mathbf{y}),\quad \mathbf{x}\in A_p^+.\tag{34}$$

The integral equations involved in (33) can be solved for low frequencies by the use of the perturbation technique as discussed in the last section, and the solution for Δu_i^{p0} is given by eqns (11)–(16). On the other hand, eqn (34) cannot be solved alone since both Δu_i^{pq} and Δu_i^{p} are unknown quantities. However, if we apply the same procedure for the remaining $(N-1)$ cracks, we obtain additional equations governing Δu_i^{pq}, Δu_i^{q} $(q\neq p,\ q = 1,2,\ldots,N)$ which in principle, can be solved. Unfortunately, this procedure becomes extremely cumbersome for a large number of cracks. Here, we will not use this method. Instead, we try to solve eqn (34) in an approximate, but simple manner.

For convenience, we write eqn (34) in the form

$$C_{3ikl}\frac{\partial}{\partial x_l}\int_{A_p^+}\sigma_{ijk}^G(\mathbf{x};\mathbf{y})\Delta u_i^{pq}(\mathbf{y})n_j\,\mathrm{d}S(\mathbf{y}) = -\bar{\sigma}_{3i}(\mathbf{x}),\quad \mathbf{x}\in A_p^+,\tag{35}$$

where

$$\begin{aligned}\bar{\sigma}_{3i}(\mathbf{x}) &= C_{3ikl}\frac{\partial}{\partial x_l}\int_{A_q^+}\sigma_{ijk}^G(\mathbf{x};\mathbf{y})\Delta u_i^{q}(\mathbf{y})n_j\,\mathrm{d}S(\mathbf{y})\\ &\simeq C_{3ikl}\frac{\partial}{\partial x_l}\sigma_{ijk}^G(\mathbf{x};\mathbf{y}^{(q)})n_j\int_{A_q^+}\Delta u_i^{q}(\mathbf{y})\,\mathrm{d}S(\mathbf{y}),\end{aligned}\tag{36}$$

in which $\mathbf{y}^{(q)}$ denotes the position vector of the center of the q-th crack. The tractions $-\bar{\sigma}_{3i}$ can be interpreted as the tractions on the surface of the pth crack, induced by a system of continuously distributed dipoles over the area defined by the surface of the qth crack. Next, by the second of eqns (36), the continuously distributed dipoles of the qth crack are replaced by an approximation to their resultants at the geometrical center of the qth crack, by taking the stress Green's function outside the integral. This approximation is expected to be reasonable if the cracks are not too closely spaced. The crack-opening volumes

$$V_i^q = \int_{A_q^+}\Delta u_i^q(\mathbf{y})\,\mathrm{d}S(\mathbf{y}),\tag{37}$$

in eqn (36) are unknown *a priori* and they have to be determined.

The integral equations involved in (35) describe the interaction of a system of dipoles with the pth crack. The crack-opening displacements Δu_i^{pq} are induced by the surface tractions on the qth crack, $-\bar{\sigma}_{3i}$, which have the same amplitude but opposite sign as the stresses on $A_p^{\pm}$, produced by a system of dipoles in the absence of the pth crack. To handle eqn (35), it is convenient to rewrite $\bar{\sigma}_{3i}$ in the form

$$\bar{\sigma}_{3i} = \sigma_{3i}^{u}V_u^q = \sigma_{3i}^{1}V_1^q+\sigma_{3i}^{2}V_2^q+\sigma_{3i}^{3}V_3^q,\tag{38}$$

where V_i^q are the crack-opening volumes of the qth crack defined by eqn (37), and σ_{3i}^{u} are given by

$$\sigma_{3t}^{u} = C_{3tkl}\frac{\partial}{\partial x_l} T_{uk}^{G}(\mathbf{x};\mathbf{y}^{(q)}), \tag{39}$$

$$T_{uk}^{G} = \sigma_{ujk}^{G} n_j. \tag{40}$$

The decomposition in eqn (38) allows us to use the superposition principle to obtain the solution for Δu_i^{pq}. If α_{iu}^{pq} are the crack-opening displacements of the pth crack caused by the tractions $-\sigma_{3t}^{u}$ $(t, u = 1, 2, 3)$, that is to say if α_{iu}^{pq} are solutions of the integral equations

$$C_{3tkl}\frac{\partial}{\partial x_l}\int_{A_q^+} \sigma_{ijk}^{G}(\mathbf{x};\mathbf{y})\alpha_{iu}^{pq}(\mathbf{y})n_j \, \mathrm{d}S(\mathbf{y}) = -\sigma_{3t}^{u}(\mathbf{x}), \quad u = 1, 2, 3, \tag{41}$$

then the solution to Δu_i^{pq} can be written as

$$\Delta u_i^{pq} = \alpha_{iu}^{pq} V_u^q, \tag{42}$$

where q indicates the qth crack and no summation over repeated q is taken. In general, the tractions $\sigma_{3t}^{u}(\mathbf{x})$ induced by dipoles on the pth crack are not uniform. To make our analysis as simple as possible, we replace $\sigma_{3t}^{u}(\mathbf{x})$ by uniformly distributed tractions on $A_p^{\pm}$ with magnitudes equal to the values of $\sigma_{3t}^{u}(\mathbf{x})$ at the geometrical center, $\mathbf{x}^{(p)}$, of the pth crack

$$\sigma_{3t}^{u}(\mathbf{x}) \simeq \sigma_{3t}^{u}(\mathbf{x}^{(p)}). \tag{43}$$

With this approximation, the boundary integral equations of (43) have been solved for low frequencies by the perturbation technique outlined in the last section. The solutions for α_{iu}^{pq} have the same forms, eqns (11)–(16), as for the case of incident waves. The coefficients occurring in (11)–(16) are different, but they are not given here for the sake of brevity.

In summary, the crack-opening displacements Δu_i^p of eqn (32) can be approximated by

$$\Delta u_i^p \simeq \Delta u_i^{p0} + \sum_{\substack{q=1\\ q\neq p}}^{N} \alpha_{iu}^{pq} V_u^q, \tag{44}$$

where V_u^q still remains unknown. Integration of eqn (44) over A_p^+ yields, however, the corresponding approximations for the crack-opening volume

$$V_i^p \simeq V_i^{p0} + \sum_{\substack{q=1\\ q\neq p}}^{N} \beta_{iu}^{pq} V_u^q, \tag{45}$$

in which

$$\beta_{iu}^{pq} = \int_{A_p^+} \alpha_{iu}^{pq}(\mathbf{y})\, \mathrm{d}S(\mathbf{y}) \tag{46}$$

are the crack-opening volumes of the pth crack, due to the tractions σ_{3t}^{u} produced by dipoles.

It is still too complicated to find Δu_i for all cracks. A natural way instead is to determine the average crack-opening displacements $\langle \Delta u_i \rangle$, as well as certain associated quantities. In the usual manner the average of a random function $f(x_1, x_2, \ldots, x_m)$, which is dependent on m random variables x_i $(i = 1, 2, \ldots, m)$, is defined as

$$\langle f\rangle = \int_{x_1}\int_{x_2}\cdots\int_{x_m} f(x_1,x_2,\ldots,x_m)p(x_1,x_2,\ldots,x_m)\,\mathrm{d}x_1\,\mathrm{d}x_2\ldots\mathrm{d}x_m, \tag{47}$$

where $p(x_1,x_2,\ldots,x_m)$ is the probability density function satisfying the normalization condition

$$\int_{x_1}\int_{x_2}\cdots\int_{x_m} p(x_1,x_2,\ldots,x_m)\,\mathrm{d}x_1\,\mathrm{d}x_2\ldots\mathrm{d}x_m = 1. \tag{48}$$

The average of Δu_i^p can then be written from eqn (44) as

$$\langle\Delta u_i^p\rangle = \Delta u_i^{p0} + \sum_{\substack{q=1\\q\neq p}}^{N}\langle\alpha_{iu}^{pq}V_u^q\rangle. \tag{49}$$

In what follows, we assume that all cracks are identical (with radius a) and parallel. We further assume that the cracks are randomly distributed so that all positions of the cracks are equally probable. Under these assumptions, we can approximate α_{iu}^{pq} and V_u^q as two independent variables, so that

$$\langle\alpha_{iu}^{pq}V_u^q\rangle \simeq \langle\alpha_{iu}^{pq}\rangle\langle V_u^q\rangle. \tag{50}$$

In addition, since all cracks are identical and parallel, the following equality can be used

$$\langle V_u^q\rangle = \langle V_u^p\rangle. \tag{51}$$

Thus, eqn (49) can be recast into the form

$$\langle\Delta u_i\rangle = \Delta u_i^0 + n\langle\alpha_{iu}\rangle\langle V_u\rangle, \tag{52}$$

where n is the number of cracks per unit volume, and the superscripts p and pq have been omittted for simplicity.

Integration of (52) over A_p^+ results in

$$\langle V_i\rangle = V_i^0 + n\langle\beta_{iu}\rangle\langle V_u\rangle, \tag{53}$$

in which

$$\langle\beta_{iu}\rangle = \int_{A_p^+}\langle\alpha_{iu}(\mathrm{y})\rangle\,\mathrm{d}S(\mathrm{y}). \tag{54}$$

Equation (53) can be rewritten as

$$\langle V_u\rangle = A_{iu}^{-1}V_i^0. \tag{55}$$

Here A_{iu}^{-1} denotes the inverse matrix of A_{iu} which is given by

$$A_{iu} = \delta_{iu} - n\langle\beta_{iu}\rangle. \tag{56}$$

Clearly, eqn (53) can also be established by averaging eqn (45) and by using similar approximations to (50) and (51). Substitution of eqn (55) into (52) yields the following expression for the average crack-opening displacements:

$$\langle \Delta u_i \rangle = \Delta u_i^0 + n\langle \alpha_{iu} \rangle A_{iu}^{-1} V_i^0. \tag{57}$$

We mention again that the average crack-opening displacements of an arbitrarily selected crack can be split approximately into two parts, as given by eqn (57). The first part represents the crack-opening displacements of the reference crack caused by the incident wave in the absence of all other cracks, while the second part describes the interaction effects of the cracks on the crack-opening displacements of this reference crack. It follows that the average forward scattering amplitude for incidence of an L-wave on this crack can also be split into two terms

$$\langle F_R \rangle = F_R^0 + \langle F_R^* \rangle \tag{58}$$

where F_R^0 is given by eqn (28) and eqn (29), while $\langle F_R^* \rangle$ can be obtained by substituting the second term of eqn (57) into eqns (23), (26) and (27). For $\phi = 0$, this yields

$$\langle F_R^* \rangle = -\frac{i(k_L a)a^2}{3\pi}\left\{\frac{(1-2\kappa^2 \sin^2\theta)}{1-\kappa^2} F_1^* \langle \sigma_{33}'' \rangle - \frac{4\kappa^2 \sin 2\theta}{3-2\kappa^2} F_2^* \langle \sigma_{31}'' \rangle \right\} n A_{iu}^{-1} V_i^0. \tag{59}$$

where σ_{31}'', σ_{33}'' are defind by eqn (39), and F_α^* is given by

$$F_\alpha^* = \bar{a}_\alpha^0 - \frac{(k_L a)^2}{10\kappa^2}(\bar{a}_\alpha^0 \kappa^2 \sin^2\theta + 2\bar{a}_\alpha^1 \kappa \sin\theta + 5\bar{a}_\alpha^2 + \bar{a}_\alpha^3 + \bar{a}_\alpha^4) - \frac{i(k_L a)^3}{6\kappa^3}\bar{a}_\alpha^5 + O[(k_L a)^4]. \tag{60}$$

The coefficients $\bar{a}_\alpha^i$ $(i = 0, 1, \ldots, 5;\ \alpha = 1, 2)$ are listed in Appendix. C. The quantities V_i^0, $\langle \beta_{iu} \rangle$ and A_{iu}^{-1} can be calculated by substituting Δu_i^0 into (37), $\langle \alpha_{iu} \rangle$ into (54), and by subsequently using eqn (56).

4. EFFECTIVE WAVE VELOCITY AND ATTENUATION

For elastic wave propagation in a cracked solid, the wave velocity is frequency dependent and the amplitude of the wave decays with advancing distance in the propagation direction. A rigorous theory for the determination of the phase velocity and the coefficient of attenuation is not yet available for the general case. In our analysis, the well established approach of Foldy (1945) and Lax (1952) for elastic wave propagation in solids containing distributed voids or inclusions, is applied in a further improved form. It is assumed that no correlations between individual scatterers exist. The effective wavenumber $\bar{k}_L$, according to this approach, can then be written as

$$(\bar{k}_L a)^2 = (k_L a)^2 + 4\pi\varepsilon \langle F_R(\bar{k}_L a) \rangle, \tag{61}$$

where a is the radius of the penny-shaped cracks, k_L is the wavenumber of the L-wave in the uncracked medium, $\langle F_R(\bar{k}_L a) \rangle$ is the average, forward scattered L-wave amplitude, and ε is the crack-density parameter defined by

$$\varepsilon = na^3, \tag{62}$$

in which n represents the number of cracks per unit volume. In general, eqn (61) has to be solved by iteration since (61) is an implicit equation for the determination of $\bar{k}_L a$. As a reasonable approximation to eqn (61), the following equation, due to Foldy (1945), is used in the present analysis

$$(\bar{k}_L a)^2 = (k_L a)^2 + 4\pi\varepsilon\langle F_R(k_L a)\rangle. \tag{63}$$

The simple form of eqn (63) allows us to calculate the complex wavenumber $\bar{k}_L a$ without iteration. The real and imaginary parts of $\bar{k}_L a$ are related to the effective wave velocity and the wave attenuation by

$$\mathrm{Re}\left(\frac{\bar{k}_L a}{k_L a}\right) = \frac{c_L}{\bar{c}_L}, \tag{64}$$

$$\mathrm{Im}\,(\bar{k}_L a) = \frac{a}{2}\alpha, \tag{65}$$

where c_L is the L-wave velocity in the uncracked medium, $\bar{c}_L$ is the L-wave velocity in the cracked medium, and α is the coefficient of attenuation.

In the standard approximation, $\langle F_R\rangle$ is replacd by F_R^0/a where F_R^0 is given by eqn (59). This means that the cracks do not have any interaction. Here we modify this approximation by setting

$$\langle F_R\rangle = F_R^0/a + \langle F_R^*\rangle/a, \tag{66}$$

where $\langle F_R^*\rangle$ is given by eqn (59) and eqn (60). Substituting eqn (66) into eqn (63) leads to

$$(\bar{k}_L a)^2 = (k_L a)^2 + 4\pi\varepsilon(F_R^0/a) + 4\pi\varepsilon(F_R^*/a). \tag{67}$$

Because interaction effects between cracks are included in eqn (67), it is believed that the modified approximation is better than the standard one, especially for moderate and larger crack densities. In fact, the third term on the right-hand side of eqn (67) is a higher order term in ε

$$4\pi\varepsilon(F_R^*/a) \sim \varepsilon^2, \tag{68}$$

since F_R^* is proportional to ε [see eqn (59)]. For small ε, this term can be ignored in comparison with the second term of eqn (67). However, for moderate or large ε, the contribution of this term may be of importance.

5. NUMERICAL RESULTS AND DISCUSSIONS

Numerical calculations based on eqn (67) have been carried out for a solid permeated by parallel penny-shaped cracks. Poisson's ratio of the uncracked material was chosen as 1/3. The probability density p is a function of the random variables R, β, γ which describe the relative crack positions. Thus, $p(R, \beta, \gamma)$ represents the probability density of finding a crack with the center defined by the spherical coordinates (R, β, γ), see Fig. 3. In this paper

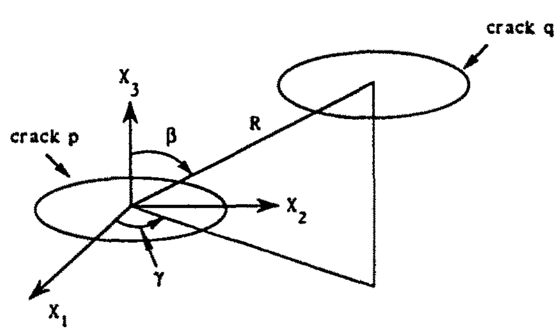

Fig. 3. Relative position of two parallel cracks.

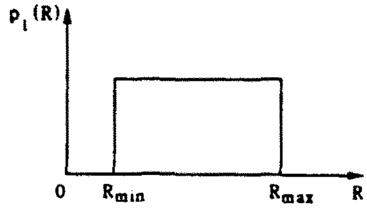

Fig. 4. The distribution function $p_1(R)$.

we consider the case that the crack center distance R and the relative crack position angles β, γ are randomly independent, so that

$$p(R, \beta, \gamma) = p_1(R)p_2(\beta, \gamma). \tag{69}$$

In the present paper, $p_1(R)$ is selected as a uniform distribution function with $R_{min} = 2.5a$ and $R_{max} = 4.5a$ (see Fig. 4), i.e.

$$p_1(R) = \begin{cases} \dfrac{1}{R_{max} - R_{min}}, & R_{min} \leqslant R \leqslant R_{max}, \\ 0 & \text{otherwise}, \end{cases} \tag{70}$$

while $p_2(\beta, \gamma)$ is taken to be completely random, i.e.

$$p_2(\beta, \gamma) = \frac{1}{2\pi^2}, \quad 0 \leqslant \beta \leqslant 2\pi, \quad 0 \leqslant \gamma \leqslant \pi. \tag{71}$$

With this specification of the probability density function, the average of a quantity can be calculated by using eqn (47).

Figure 5 shows the dependence of the velocity ratio $\bar{c}_L/c_L$ on the crack-density parameter ε for several dimensionless wavenumbers $k_T a$, where k_T is the wavenumber of transverse waves in the uncracked medium. The case $\varepsilon = 0$ corresponds to a medium without cracks, when $\bar{c}_L/c_L$ is unity. The presence of cracks reduces the wave velocity as expected. The effective wave velocity decreases with increasing crack density. For fixed crack density, $\bar{c}_L$ decreases as $k_T a$ increases from 0.3 to 0.9. Calculations based on the standard approximation, that is without the last term in eqn (67), have also been carried out. It was found that the standard approach generally underestimates the effective wave velocity. However, the differences in $\bar{c}_L/c_L$ from both approaches are so small that they

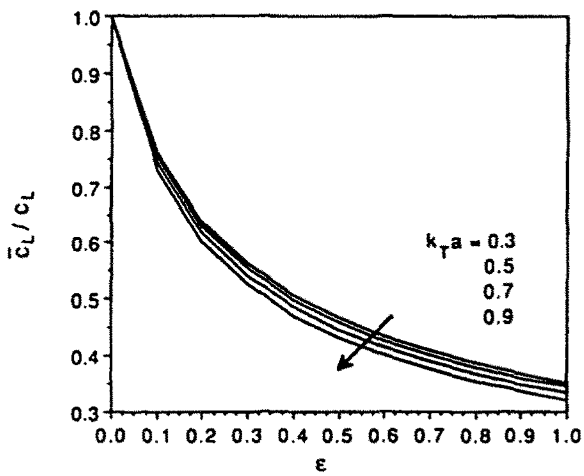

Fig. 5. Phase velocity versus crack density for normal incidence of an L-wave.

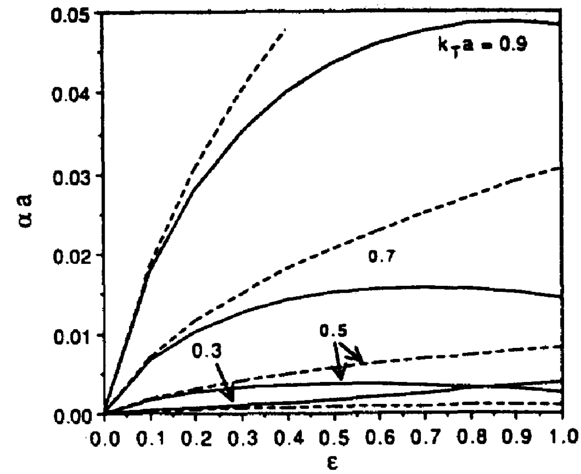

Fig. 6. Coefficient of attenuation versus crack density for normal incidence of an L-wave; -----: standard approach, ———: improved approach.

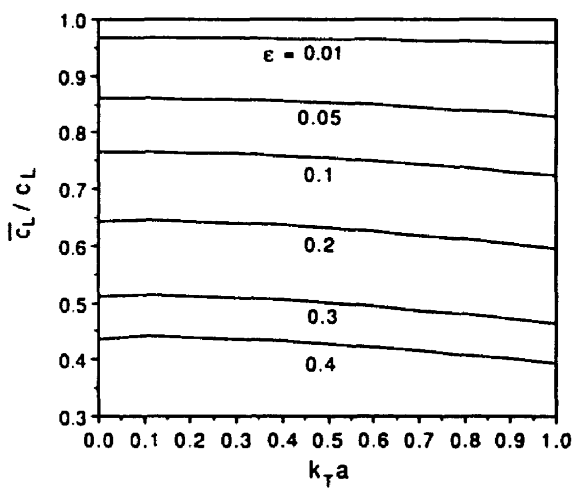

Fig. 7. Phase velocity versus dimensionless wavenumber for normal incidence of an L-wave.

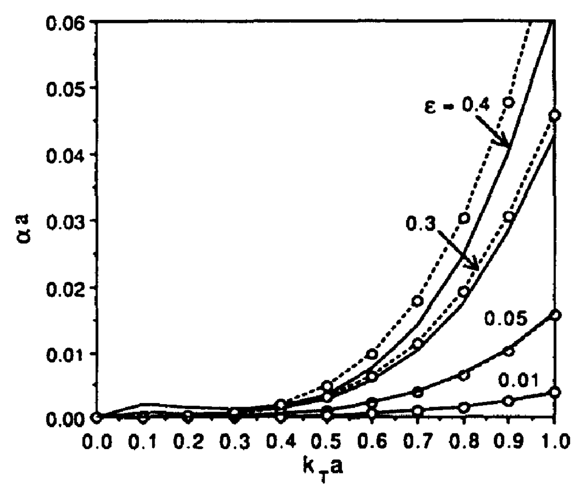

Fig. 8. Coefficient of attenuation versus dimensionless wavenumber for normal incidence of an L-wave; --○--○--○--: standard approach, ———: improved approach.

cannot be distinguished graphically, at least in the frequency range considered here. Thus, only the results of the modified approximation are shown in Fig. 5.

The coefficient of attenuation of L-waves is shown in Fig. 6 versus the crack density ε. Both results from the standard and the modified approximation are shown. For small wave numbers, for example $k_T a = 0.3$, the standard approximation underestimates the attenuation, while for larger wavenumbers it overestimates the attenuation. For the case of small crack density both results agree very well, while for increasing crack density, the difference beteen the results for the two approaches becomes larger and larger.

The dependence of the effective wave velocity and the attenuation on the dimensionless wavenumber is shown in Fig. 7 and Fig. 8. The effective wave velocity decreases with increasing wavenumber in the frequency range considered, though this change is not substantial. The coefficient of attenuation increases as $k_T a$ increases. The results show again that the standard independent scatterer approximation and the modified one yield the same results for dilute crack distribution, while for dense crack distributions the standard approach underestimates the attenuation for low frequencies (say $k_T a < 0.4$) and overestimates the attenuation for high frequencies.

Figure 9 shows the variation of the effective wave velocity with the angle of incidence, for several selected values of ε and $k_T a$. The effective wave velocity is smallest for $\theta = 0^\circ$ (normal incidence of the L-wave) and largest for $\theta = 90^\circ$ (grazing incidence of the L-wave). It is interesting to note that even when the L-wave propagates parallel to the cracks, a

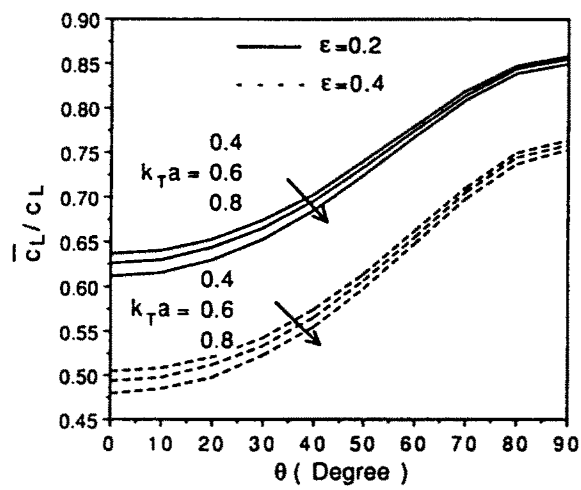

Fig. 9. Phase velocity versus the angle of incidence for an L-wave.

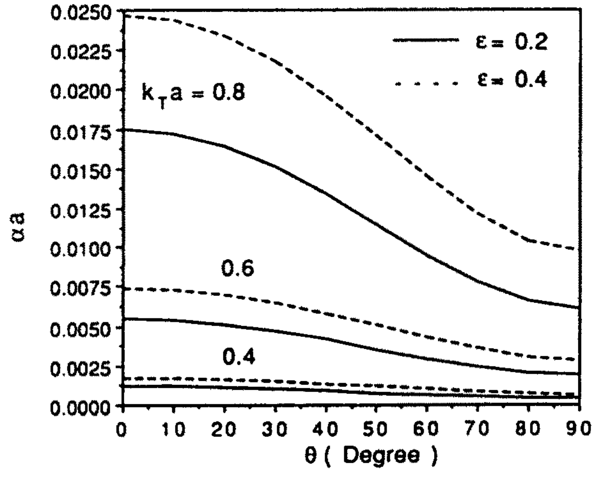

Fig. 10. Coefficient of attenuation versus the angle of incidence for an L-wave.

reduction in the effective wave velocity is induced. In Fig. 10, the attenuation is plotted versus the angle of incidence of the L-wave. In contrast to the effective wave velocity, the attenuation has a maximum at $\theta = 0^\circ$, and it decreases with increasing θ to a minimum at $\theta = 90^\circ$. As expected, the cracks cause maximum effects of interfering with wave motion when the surfaces of the cracks are perpendicular to the direction of wave propagation.

In concluding, we note that a limitation of the theory presented herein is in the range of validity of the low-frequency scattering theory for a single crack. The results of Fig. 2 suggest that this theory is valid for $k_T a < 1.0$. Hence, for illlustrative purposes, the results are presented in Figs 5–10 for $0 \leqslant k_T a \leqslant 1$. The general approach of this paper can, however, also be used for intermediate and high frequencies, in conjunction with a suitable numerical technique (BEM, FEM, etc.) for calculating the crack-opening displacements.

Acknowledgements—This work was carried out in the course of research for Contract DEFG02-86-ER13484 with the Department of Energy, Office of Basic Energy Sciences, Engineering Research Program. Support from the Florida State University Supercomputer Computations Research Institute, which is partially funded by the U.S. Department of Energy through Contract No. DE-FC05-85ER250000, is also acknowledged.

REFERENCES

Anderson, D. L., Minster, B. and Cole, D. (1974). The effect of oriented cracks on seismic velocities. *J. Geophys. Res.* **79**, 4011–4015.

Bose, S. K. and Mal, A. K. (1974). Elastic waves in a fiber-reinforced composite. *J. Mech. Phys. Solids* **22**, 217–229.

Budreck, D. E. and Achenbach, J. D. (1988). Scattering from three-dimensional planar cracks by the boundary integral equation method. *J. Appl. Mech.* **55**, 405–412.

Chatterjee, A. K., Mal, A. K., Knopoff, L. and Hudson, J. A. (1980). Attenuation of elastic waves in a cracked, fluid-saturated solid. *Math. Proc. Camb. Phil. Soc.* **88**, 547–561.

Datta, S. K. (1977). A self-consistent approach to multiple scattering of elastic waves. *J. Appl. Mech.* **44**, 657–662.

Datta, S. K., Ledbetter, H. M., Shindo, Y. and Shah, A. H. (1980). Phase velocity and attenuation of plane elastic waves in a particle-reinforced composite medium. *Wave Motion* **10**, 171–182.

Foldy, L. L. (1945). Multiple scattering theory of waves. *Phys. Rev.* **67**, 107–119.

Garbin, H. D. and Knopoff, L. (1973). The compressional modulus of a material permeated by a random distribution of circular cracks. *Q. Appl. Math.* **30**, 453–464.

Garbin, H. D. and Knopoff, L. (1975a). The shear modulus of a material permeated by a random distribution of free circular cracks. *Q. Appl. Math.* **33**, 296–300.

Garbin, H. D. and Knopoff, L. (1975b). Elastic moduli of a medium with liquid-filled cracks. *Q. Appl. Math.* **33**, 301–303.

Gubernatis, J. E. and Domany, E. (1984). Effects of microstructure on the speed and attenuation of elastic waves in porous materials. *Wave Motion* **6**, 579–589.

Krenk, S. and Schmidt, H. (1982). Elastic wave scattering by a circular crack. *Phil. Trans. R. Soc. London* **A308**, 167–198.

Lax, M. (1952). Multiple scattering of waves II. Effective field in dense systems. *Phys. Rev.* **85**, 621–629.

Lin, W. and Keer, L. M. (1987). Scattering by a planar three-dimensional crack. *J. Acoust. Soc. Am.* **82**, 1442–1448.

Mal, A. K. (1970). Interaction of elastic waves with a penny-shaped crack. *Int. J. Engng Sci.* **8**, 381–388.

Mal, A. K. (1972). A note on the low frequency diffraction of elastic waves by a Griffith crack. *Int. J. Engng Sci.* **10**, 609–612.

Martin, P. A. and Wickham, G. R. (1983). Diffraction of elastic waves by a penny-shaped crack: analytical and numerical results. *Proc. R. Soc. London Ser. A* **390**, 91–129.

McCarthy, M. F. and Carroll, M. M. (1984). Wave propagation in randomly cracked media. In *Wave Propagation in Homogeneous Media and Ultrasonic Nondestructive Evaluation* (Edited by G. C. Johnson), Vol. 62, pp. 141–153. ASME, New York, U.S.A.

Nishimura, N. and Kobayashi, S. (1989). A regularized boundary integral equation method for elastodynamic crack problems. *Comp. Mech.* **4**, 319–328.

O'Connell, R. J. and Budiansky, B. (1974). Seismic velocities in dry and saturated cracked solids. *J. Geophys. Res.* **79**, 5412–5426.

Piau, M. (1979). Attenuation of a plane compressional wave by a random distribution of thin circular cracks. *Int. J. Engng Sci.* **17**, 151–167.

Piau, M. (1980). Crack-induced anisotropy and scattering in stressed rocks: effective elastic moduli and attenuation. *Int. J. Engng Sci.* **18**, 549–568.

Robertson, I. A. (1967). Diffraction of a plane longitudinal wave by a penny-shaped crack. *Proc. Camb. Phil. Sol.* **63**, 229–238.

Roy, A. (1987). Diffraction of elastic waves by an elliptic crack-II. *Int. J. Engng Sci.* **25**, 155–169.

Sayers, C. M. and Smith, R. L. (1983). Ultrasonic velocity and attenuation in an epoxy matrix containing lead inclusions. *J. Phys. D: Appl. Phys.* **16**, 1189–1194.

Sotiropoulos, D. A. and Achenbach, J. D. (1988). Reflection of elastic waves by a distribution of coplanar cracks. *J. Acoust. Soc. Am.* **84**, 752–759.

Twersky, V. (1962). On scattering of waves by random distributions. I. Free-space scatterer formalism. *J. Math. Phys.* **3**, 700–715.
Varadan, V. K., Ma, Y. and Varadan, V. V. (1985). A multiple scattering theory for elastic wave propagation in discrete random medium. *J. Acoust. Soc. Am.* **77**, 375–385.
Varadan, V. K., Varadan, V. V. and Pao, Y. H. (1978). Multiple scattering of elastic waves by cylinders of arbitrary cross section. I. SH-waves. *J. Acoust. Soc. Am.* **63**, 1310–1319.
Waterman, P. C. and Truell, R. (1961). Multiple scattering of elastic waves. *J. Math. Phys.* **2**, 512–537.

APPENDIX A: THE STRESS GREEN'S FUNCTION

The stress Green's function $\sigma^G_{ijk}(\mathbf{x};\mathbf{y})$ denotes the stress components at $\mathbf{x}$ caused by a point force of unit amplitude in the k direction, applied at $\mathbf{y}$. For a homogeneous, isotropic, linearly elastic and unbounded solid the stress Green's function has the following explicit form

$$\sigma^G_{ijk} = \frac{2}{k_T^2}(G^T - G^L)_{,ijk} + (1-2\kappa^2)\delta_{ij}G^L_{,k} + \delta_{ik}G^T_{,j} + \delta_{jk}G^T_{,i}, \tag{A1}$$

where

$$G^\alpha = \exp(ik_\alpha R)/4\pi R, \quad \alpha = \mathrm{L},\mathrm{T}, \tag{A2}$$

$$R = |\mathbf{x}-\mathbf{y}|, \tag{A3}$$

$$\kappa = k_L/k_T, \tag{A4}$$

and k_L, k_T are the wave numbers of longitudinal and the transverse waves, respectively.

APPENDIX B: THE COEFFICIENTS a^l_α OF EQN (29)

The coefficients a^l_α of eqn (29) are

$$a^0_1 = 1, \tag{B1}$$

$$a^1_1 = 2\kappa\sin\theta, \tag{B2}$$

$$a^2_1 = -\tfrac{1}{6}[4h_0(\kappa) - \kappa^2\sin^2\theta], \tag{B3}$$

$$a^3_1 = \tfrac{1}{45}[5h_0(\kappa) + 22\kappa^2\sin^2\theta], \tag{B4}$$

$$a^4_1 = \tfrac{1}{45}[5h_0(\kappa) - 2\kappa^2\sin^2\theta], \tag{B5}$$

$$a^5_1 = -\frac{2}{3\pi}h_1(\kappa), \tag{B6}$$

$$a^0_2 = -1, \tag{B7}$$

$$a^1_2 = \frac{4\kappa(3-2\kappa^2)}{3(6\kappa^2-7)}, \tag{B8}$$

$$a^2_2 = \frac{1}{16}\left\{\pi^2 b_1 + \frac{4\kappa}{45(\kappa^2-1)}[(7\kappa^2-6)b_2 + (\kappa^2-1)(4\kappa^2+3)b_3]\right\}, \tag{B9}$$

$$a^3_2 = \frac{2}{45(1-\kappa^2)}[(9-7\kappa^2)b_2 + 2\kappa^2(\kappa^2-1)b_3], \tag{B10}$$

$$a^4_2 = \frac{1}{45(1-\kappa^2)}[(4\kappa^2-3)b_2 + 2(8\kappa^2-15)(\kappa^2-1)b_3], \tag{B11}$$

$$a^5_2 = \frac{16(3+2\kappa^3)}{15\pi(3-2\kappa^2)}, \tag{B12}$$

in which

$$b_1 = \frac{2+\kappa^4}{2(3-2\kappa^2)}, \tag{B13}$$

$$b_2 = \frac{4+3\kappa^4}{8(2\kappa^2-3)} - \kappa^2\sin^2\theta, \tag{B14}$$

$$b_3 = \frac{4+\kappa^4}{8(2\kappa^2-3)}, \tag{B15}$$

$$h_0(\kappa) = \frac{3(1-\kappa^2)^2+2\kappa^2}{2(1-\kappa^2)}, \tag{B16}$$

$$h_1(\kappa) = \frac{32\kappa^5 - 40\kappa^3 + 15\kappa + 8}{5(1-\kappa^2)}. \tag{B17}$$

APPENDIX C: THE COEFFICIENTS $\bar{a}_\alpha^i$ OF EQN (58)

The coefficients $\bar{a}_\alpha^i$ of eqn (58) are:

$$\bar{a}_1^0 = 1, \tag{C1}$$

$$\bar{a}_1^1 = 0, \tag{C2}$$

$$\bar{a}_1^2 = -4h_0(\kappa)/9, \tag{C3}$$

$$\bar{a}_1^3 = \bar{a}_1^4 = h_0(\kappa)/9, \tag{C4}$$

$$\bar{a}_1^5 = -\frac{2}{3\pi} = h_1(\kappa), \tag{C5}$$

$$\bar{a}_2^0 = -1, \tag{C6}$$

$$\bar{a}_2^1 = 0, \tag{C7}$$

$$\bar{a}_2^2 = \frac{1}{16}\left\{\pi^2 b_1 + \frac{4}{45(\kappa^2-1)}\left[(7\kappa^2-6)b_2 + (\kappa^2-1)(4\kappa^2+3)b_3 + \tfrac{1}{2}(2\kappa^2-3)(2\kappa^2-1)b_4\right]\right\}, \tag{C8}$$

$$\bar{a}_2^3 = \frac{2}{45(1-\kappa^2)}\left[(9-7\kappa^2)b_2 + 2\kappa^2(\kappa^2-1)b_3 + \tfrac{1}{2}(2\kappa^2-1)(8\kappa^2-9)b_4\right], \tag{C9}$$

$$\bar{a}_2^4 = \frac{1}{45(1-\kappa^2)}\left[(4\kappa^2-3)b_2 + 2(8\kappa^2-15)(\kappa^2-1)b_3 + \tfrac{1}{2}(2\kappa^2-1)(8\kappa^2-9)b_4\right], \tag{C10}$$

$$\bar{a}_2^5 = \frac{16(3+2\kappa^5)}{15\pi(3-2\kappa^2)^2}, \tag{C11}$$

where $h_0(\kappa)$, $h_1(\kappa)$, b_1, b_2 and b_3 can be found in Appendix B, while b_4 is given by

$$b_4 = \frac{\kappa^4}{4(2\kappa^2-3)} \cdot \frac{\sigma'_{12}}{\sigma'_{11}}. \tag{C12}$$